

## Route-planning in output-material-flow arable farming operations aiming for soil protection

Santiago Focke Martinez<sup>1</sup> and Joachim Hertzberg<sup>1,2</sup>

**Abstract:** This paper presents two approaches for route planning in output-material-flow arable farming: one for time optimization and one for soil protection. The two approaches were used to plan the routes of one harvester and one transport vehicle performing a harvesting operation in a test field, and were compared by analyzing the operation duration, travel distance, and area driven over by the machines. The results show the benefits and drawbacks of planning the machine routes using the proposed method for soil protection: the plans can reduce the impact of driving over the soil, but it can result in higher operation durations and traveled distances.

**Keywords:** route planning, precision farming, smart farming

### 1 Introduction

In the last years, technologies and methods have been developed aiming to improve the efficiency of arable farming processes, addressing topics such as operational costs, energy consumption, traffic intensity in the field, and soil compaction. This tendency has been driven by the introduction of more advanced, and at times heavier and larger, machinery in the field. One of the focus research topics is route planning, which aims to generate suitable driving paths for the machines following some target optimization criteria and the specific requirements and characteristics of the farming operations [Mo20; Ed17; NZ20]. Current research includes operations involving input-, output-, and neutral-flow operations, with both capacitated and non-capacitated machines.

This paper presents two of the approaches for path-search optimization used in the route planning tool presented in [Fo21], namely operation-time optimization and soil protection. This tool was developed to process the field geometries, generate the paths that the primary machines working the field need to follow to cover the complete area, and plan the transit of primary and service machines (in the spatio-temporal domain) following a specified optimization criterion while considering the capacity constraints of the operations. This paper presents a short overview of the route planning tool, followed by the details of the two proposed optimization approaches. Next, exemplary results and comparisons between the two approaches are shown. Finally, limitations, and conclusions are presented.

---

<sup>1</sup> German Research Centre for Artificial Intelligence (DFKI), PBR, Berghoffstraße 11, 49090 Osnabrück, santiago.focke@dfki.de

<sup>2</sup> University of Osnabrück, Berghoffstraße 11, 49090 Osnabrück, joachim.hertzberg@uos.de

## 2 Methods

The tool used for the overall planning process was previously presented in [Fo21]. Given a field, a working group of machines, and some operation and planning parameters, this tool generates the field geometries and machine routes for a target output-material-flow operation (e.g., harvesting). Two types of machines are considered: a primary machine (PM), which is the one performing the main work in the field (e.g., harvester); and service units (SU), which cooperate with the primary machine in the process (e.g., transport vehicles). The service units are introduced in the operation when the PM has no capacity, hence the need for these units to transport the biomass. Initially, the field geometries are generated, which include the boundaries between the (surrounding) headland of the field and the inner-field (main) region, as well as the headland and inner-field tracks to be followed by the PM to cover the field's working area (Fig. 1(a)). Based on these boundaries and tracks, the so-called base route of the PM is computed, which represents the route that the PM would follow to cover the field without considering the capacity constraints or unloading activities. The base route holds information about the amount of biomass to be extracted from the field and the initial timestamps of when an area will be worked. Next, a graph is constructed based on the field geometries (incl. boundaries, tracks, and access points), the base route, and the locations of the facilities where the biomass can be unloaded (Fig. 1(b)). Finally, the process routes are computed. For this final step, the process is divided into sub-processes, derived from the working windows of the capacitated machines. These working windows are computed based on the capacity constraints of the machines and the amount of biomass in the field, and each one comprises three route segments: 1) driving while working the field until the machine's capacity is reached (e.g., harvesting an area and, in the case of the SUs, overloading the biomass from the PM to the SU); 2) driving to an unloading facility to deposit the biomass; and 3) driving to the next working/overloading point (if needed). The first route segment of the window (referred to as working segment) will be dictated by the corresponding segment of the base route, whereas the planning of the second and third segments (referred to as transit segments) is done using an A\* search on the generated graph based on the edge-cost definitions given by the desired optimization criterion, while ensuring that the machines will not drive over unworked areas.

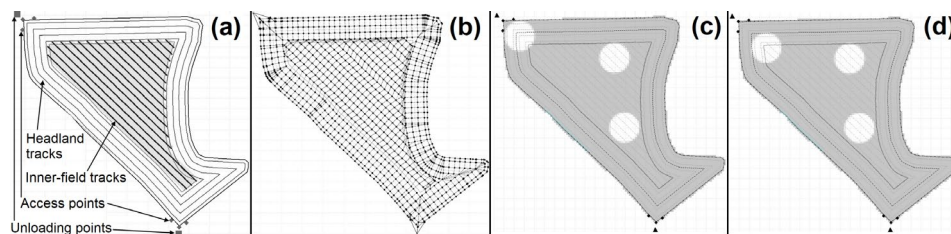


Fig. 1: (a) Test field: headland and inner-field regions with their respective tracks; (b) Graph; (c) Soil-cost gridmap CM1; (d) Soil-cost gridmap CM2

This paper presents two different approaches for the definitions of the edge-costs used in the planning of the transit route segments: one aims to minimize the overall operation time; the other one aims to protect the soil during transit. The edge cost (EC) for operation-time optimization ( $T_{OPT}$ ) is given by

$$EC = t_d + K_{wt} \cdot t_w + P + K_d \cdot d, \quad (1)$$

where  $t_d$  is the time spent driving over the edge (in seconds),  $t_w$  is the time the machine must wait to drive over the edge (in seconds),  $K_{wt}$  is the waiting time coefficient,  $d$  is the distance travelled in the edge (in meters),  $K_d = 0.001$  is the distance coefficient, and

$$P = \begin{cases} 0 & ; \text{Nomal edge} \\ K_{TC} \cdot t_d & ; \text{Edge crossing tracks} \\ K_{BC} \cdot t_d & ; \text{Edge in the field boundary} \end{cases}, \quad (2)$$

is the penalty cost for driving over special edges, where  $K_{TC}$  is the penalty coefficient for edges that connect vertices belonging to different tracks, and  $K_{BC}$  is the penalty coefficient for edges located in the field's boundary. Both penalty coefficients can be set by the user depending on the operation preferences. For instance,  $K_{TC}$  can be set based on whether it is preferred that the machines drive to the goal without changing tracks inside the field or not. Likewise,  $K_{wt}$  can be set depending on whether the time a machine is stationary and waiting for an area to become available should be considered in the cost or not.

The edge cost for soil protection ( $S_{OPT}$ ) is defined based on two main criteria: 1) reduce the amount of mass that drives over the edge throughout the operation; and 2) reduce transit over edges with high soil-cost. The edge cost is given by

$$EC = \begin{cases} K_p \cdot (d \cdot m_\Sigma \cdot (K_b + K_s \cdot c_s^2 + K_t \cdot t/d)) & ; \text{inside the field} \\ 0.1 \cdot (d + t) & ; \text{outside the field} \end{cases}, \quad (3)$$

where  $t = t_d + K_{wt} \cdot t_w$  is the time spent in the edge (in seconds),  $0 \leq c_s \leq 1$  is the soil-cost value for the area driven under the edge,  $K_b$ ,  $K_s$ , and  $K_t$  are the bias-, soil-cost-, and time- coefficients, respectively,

$$K_p = \begin{cases} 1 & ; \text{Nomal edge} \\ 1 + K_{TC} & ; \text{Edge crossing tracks} \\ 1 + K_{BC} & ; \text{Edge in the field boundary} \end{cases}, \quad (4)$$

is the penalty factor for driving over special edges, and

$$m_\Sigma = m + K_w \cdot \sum m_{prev}, \quad (5)$$

where  $m$  is the mass (in kg) of the machine planning to drive over the edge,  $\sum m_{prev}$  is the sum of the masses (in kg) of the machines planned to drive over the edge at an earlier time (i.e., corresponding to previously planned route segments), and  $K_w$  is the coefficient of the sum of previous masses. The soil-cost value  $c_s$  is obtained from a soil-cost grid-map

generated specifically for the current state of the field and is given as a planning parameter by the user. This cost-map should be generated based on factors such as the soil type, current compaction level, and moisture. More generally, it can be generated in a way that depicts the sensitive areas that should be avoided during transit. Note in (3) that, for edges corresponding to transit outside of the field, factors such as the soil state and the machine mass are not considered; however, shorter/faster paths are preferred.

To assess the proposed methods, a harvesting operation was planned for the test field in Figure 1 (area: 2.31 ha). The field has two access regions (with three access points each), connected to a corresponding unloading point located outside of the field. Additionally, two soil-cost grid-maps with cell resolution of 1 meter were generated, namely CM1 (Fig. 1(c)) and CM2 (Fig. 1(d)), where three circular regions with a high cost of  $1.0$  were added, whereas the remaining field area was left with a low cost of  $0.1$ . The difference between CM1 and CM2 lies in the location of the high-cost area near one of the access regions (closer to the access points in CM1), which correspond to an area with high potential to transit. The harvesting operations were planned with a desired headland width of 24 m, an average yield of 40 t/ha, and two machines: a non-capacitated harvester (mass: 19.6 Mg, working width: 6 m) and a transport vehicle (mass: 21.16 Mg, container capacity: 10 Mg). Four different sets of planning parameters were used to test the results: one corresponding to  $T_{OPT}$  and the other three to  $S_{OPT}$ . The cost coefficients can be seen in Table 1.  $S_{OPT-1}$  aims to balance the costs related to driving over areas with high soil-costs and driving over areas previously driven;  $S_{OPT-2}$  aims mostly to avoid as much as possible driving over areas with high soil-cost; and  $S_{OPT-3}$  aims mostly to reduce driving over already driven areas.

Optimization type	$K_{wt}$	$K_w$	$K_p$	$K_s$	$K_t$	$K_{TC}$	$K_{BC}$
$T_{OPT}$	1	--	--	--	--	2.5	15
$S_{OPT-1}$	--	0.5	0.2	3	0	2.5	50
$S_{OPT-2}$	--	0.5	0.01	3	0	2.5	50
$S_{OPT-3}$	--	0.5	0.2	0.01	0	2.5	50

Tab. 1: Cost coefficients

To compare the results, a grid-map with a resolution of 1 m was generated for each planned operation, and the routes generated for both machines were mapped into the grid-map based on the respective machine's width. This grid-map holds information about the mass driven over the area corresponding to each cell. All the cells that were driven over were used to obtain the average (*Avg*), maximum value (*Max*), and standard deviation (*SD*) of the following values: the mass driven over the cell (*MDC*), and the mass driven over the cell multiplied by the corresponding soil-cost of the cell ( $MDC \times SC$ ). Additionally, the duration and travelled distance of all plans were compared to the duration and distance resulting from the corresponding  $T_{OPT}$  plan ( $T_{diff}$  and  $D_{diff}$ , respectively).

### 3 Results

Tab. 2 shows the results for all planned operations. As expected, the duration and travelled distance for  $T_{OPT}$  is lower than for the  $S_{OPT}$  plans. Note that the differences ( $T_{diff}$ ,  $D_{diff}$ ) between  $T_{OPT}$  and  $S_{OPT-1}$  and  $S_{OPT-2}$  are much higher for CM1 than for CM2. This shows how the soil-cost-based planning is highly dependent on the soil state throughout the field, or, in other words, on the proximity of high-cost areas to areas with high transit potential (such as field access regions). These plans will search for alternative paths to avoid these costly areas, which could result in significantly higher durations and increased travel inside the field if the alternatives are limited. On the other hand, lower travel distances result in less driven area; however, this does not necessarily correspond to an overall lower negative impact on the soil.  $S_{OPT-3}$  shows the best mass distribution in the field, with low average and SD of the MDC. When considering the cells' soil-cost in addition to the mass ( $MDC \times SX$ ),  $S_{OPT-2}$  yields the best results, as it aims to decrease the total mass driven over high-cost areas. Finally, the results for  $S_{OPT-1}$  show the compromise between avoiding driving over previously driven areas and avoiding driving over high soil-cost regions.

Soil-cost gridmap	Opt. type	$T_{diff}$ [%]	$D_{diff}$ [%]	MDC [kg] (Mass driven over a cell)			MDC×SC (MDC [kg] × soilcost)		
				Avg.	Max.	SD	Avg.	Max.	SD
CM1	$T_{OPT}$	0.0	0.0	42137	389586	34861	8188	389586	19933
	$S_{OPT-1}$	6.5	4.6	43958	322216	33158	7439	186174	13097
	$S_{OPT-2}$	15.7	10.8	46442	326159	36371	7354	112484	11090
	$S_{OPT-3}$	1.9	1.2	42636	343636	32936	8228	343636	18515
CM2	$T_{OPT}$	0.0	0.0	42137	389586	34861	7681	343018	17049
	$S_{OPT-1}$	1.6	1.3	42247	266670	32807	6910	100512	10948
	$S_{OPT-2}$	2.5	2.0	42539	268231	33158	6930	100512	10926
	$S_{OPT-3}$	1.9	1.2	42634	328146	32750	7406	168536	13534

Tab. 2: Results

It is important to note that the planning process is not free of limitations [Fo21], which are reflected also in the assessment process. The route planning and assessment do not consider the complete kinematics of the machines and the location of the wheels, which are the ones in contact with the ground. Instead, in this paper, the area considered to be driven over by the machine between two route points corresponds to a rectangular projection on the ground derived from the distance between the route points and the width of the machine. Moreover, the planned routes are computed based on the geometries of the graph, which is generated based on the tracks and is a discretized version of the field. Because of this, areas between the tracks are not fully utilized during planning, for instance, in cases where the working width of the PM is higher than the base widths of the machines. For the test field, only about 80 % of the cells were considered to be overrun.

## 4 Conclusions

This paper presented two of the approaches for path-search optimization used in the planning tool from [Fo21]: one to optimize the operation duration and the other one to improve the soil protection. The two approaches were compared by analyzing the duration, travel distance, and area driven over for the planned operations. Although the presented assessment method has limitations, it exhibits the benefits and drawbacks of planning the machine routes based on the criteria used to define the edge-costs aiming for soil protection ( $S_{OPT}$ ). The results suggest that it is possible to reduce the impact of driving on the soil using the proposed method for soil protection. However, depending on the specific state of the soil and the geometries of the field, planning the routes with this method could significantly increase the process duration and travel distance of the machines, which results in higher utilization of resources (machinery, fuel, etc.). A way to mitigate this drawback is to improve the potential for alternative paths (as possible), for instance, by increasing the number of field access points. Moreover, the route planning process can be enhanced to improve the results. For instance, a track-sequence planner that considers the optimization targets can be incorporated in the process. In the case of soil protection, leaving the tracks that overlap with higher soil-cost areas to be worked towards the end of the operation would improve the drivability in the field in the early stages of the operation. Moreover, selecting a proper cost definition is a challenging task; different criteria for soil protection would result in different cost definitions and/or coefficient values. Finally, an extended assessment that considers the real driving following the planned paths, the kinematics of the wheels and corresponding wheel load on the ground, and that incorporates more complex transit and soil-impact models should be carried out.

The SOILAssist project is funded by the Federal Ministry of Education and Research (BMBF) within the framework of the BonaRes-initiative (grant no. 031B0684B). The DFKI Niedersachsen Lab (DFKI NI) is sponsored by the Ministry of Science and Culture of Lower Saxony and the VolkswagenStiftung.

### References

- [Mo20] Moysiadis, V. et.al: Mobile Robotics in Agricultural Operations: A Narrative Review on Planning Aspects. *Applied Sciences* 10/20, p. 3453, 2020.
- [Ed17] Edwards, G. et.al: Route planning evaluation of a prototype optimised infield route planner for neutral material flow agricultural operations. *Biosystems Engineering* 153/17, p. 149-157, 2017.
- [NZ20] Nilsson, R.S.; Zhou, K. Decision Support Tool for Operational Planning of Field Operations. *Agronomy* 10/20, p. 229, 2020.
- [Fo21] Focke Martinez, S. et.al: Overview of a route-planning tool for capacitated field processes in arable farming, in 41. GIL-Jahrestagung, Informations- und Kommunikationstechnologie in kritischen Zeiten, Bonn, 2021.